International Journal of Innovation Engineering and Science Research
(ISSN: 2581-4591)
www.ijiesr.com

Quad-Element MIMO Antenna with Enhanced Isolation for UWB Applications

Giday Gebrehiwot Bsrat
Andhra University College of Engineering(A)
Visakhapatnam,India

S.Aruna
Andhra University College of Engineering(A)
Visakhapatnam,India

K. Srinivasa Naik
Vignan's Institute of Information Technology,
Visakhapatnam,India

ABSTRACT

This study proposes a quad-element MIMO antenna for ultra-wide band applications. Design evolutions have been carried out in order to achieve large impedance bandwidth and good positive gain across the operating frequency range. In MIMO antenna construction, the best-performing antenna design is used as a basic radiator element. S-parameters, radiation patterns, and diversity performance findings are thus used to investigate MIMO antenna designs with various layouts.As a result, a quad-element MIMO antenna with orthogonal radiators orientation that operates in the frequency range of 3.5-11.2 GHz with >-20dB isolation in the majority of the operating band is proposed. The ECC and DG values are less than 0.006 and greater than 9.9, respectively, while the MEG and CCL are within acceptable ranges. The simulated findings agree well with the measured results.

Keywords—*Mutual couling,Envelope correlation coefficient (ECC), Diversity gain (DG), Mean effective gain (MEG), Channel capacity loss (CLL).*

I. INTRODUCTION

In modern wireless devices, because of their many advantages, microstrip antennas are the most popular antenna type. Microstrip antennas are low-profile, light-weight, simple to manufacture, and adaptable to mounting hosts, with a portable conducting patch printed on a grounded substrate. However, they naturally have a narrow bandwidth, and bandwidth improvement is usually required for many purposes. Besides, the requirements of ultra-wideband patch antennas in recent days are alarmingly increasing because of their wide frequency impedance bandwidth and solve the limitations of narrowband antennas. Ultra-wideband antennas are promising candidates for applications in UWB communications, like biomedical, military and commercial applications in general. According to the U.S FCC regulations, the spectrum of UWB covers a 3.1 to 10.6 GHz frequency bandwidth, which is intended for high-speed short-range communication [1].

Conventional microstrip patch antennas have some limitations, like narrow bandwidth, low gain and large size. Several methods of enhancing the performance of microstrip antennas have been reported in many literatures. Patch antennas with partial ground plane [1], [2], patch antenna with defected ground structure (DGS) that can be used for UWB application was proposed in [3]. The DGS significantly controls the impedance bandwidth and improves the radiation characteristics of monopole antennas by suppressing the higher modes of harmonics and reduce mutual coupling between adjacent elements[4], [5]. In, creating different-shaped slots in the ground plane can modify surface

current distribution, resulting in a change in the impedance bandwidth of a monopole, and this structure is called a defected ground structure (DGS). Using such structures, circular polarization can be achieved, multiband effect and improved radiation properties [6], [7]. On the other hand, due to the nature of forming periodic structures to possess band gap for surface wave propagation, Electromagnetic band gap structures (EBG) are also used[8], met-materials or photonic band gaps are also crucial for the impedance bandwidth and gain enhancements [9]. In a single physical package, two or more antennas can be designed for both transmission and reception applications in wireless technology. This kind of technology is known as Multiple-Input Multiple-Output (MIMO) antennas. By exploiting multiple antennas, the amount of data and range are improved compared to a single antenna using the same radio transmit power. Moreover, MIMO antennas boost link reliability and experience less fading than a single antenna system. In general, using MIMO technology, wireless capacity grows and numerous consumers can access various services at the same time too. Integration of UWB technology with MIMO techniques has become a solution to the short-range communications constraint [10], [11] which necessitates devices transmitting very small power.

Up to now, several research papers on MIMO antennas for UWB applications have been reported. Different techniques are proposed for good isolation for the reduction of mutual coupling and, as a result, to enhance the performance characteristics. In [12], a two-element UWB-MIMO antenna with >20 dB isolation over the band of 3 to 10.9GHz with a total size of 30×50×167mm^3 is proposed, to increase impedance bandwidth and improve isolation at the lower band, L-shaped open-slots are introduced in the common ground, along with a decoupling network comprised of a narrow slot and a fork-shaped slot. Additionally, a dual polarized slot antenna for ultra wideband applications with a size of 66.2 ×66.2 ×1.6 mm^3 is proposed in [13]. Better isolation > 20dB and good impedance matching are achieved by shaping the slot arms and feed section suitably and inserting narrow metallic stubs. In [14], The use of two element MIMO for UWB with reduced mutual coupling is proposed, and the middle portion of the ground structure is expanded outward to provide better isolation of > 20dB over the entire UWB with a size of 40×80×1.6mm^3. An UWB semi-ring MIMO antenna with a size of 50×90×1.52mm^3 and isolation > 10dB on the entire band is indicated in [10]. In [15], A compact two-element UWB-MIMO is reported. Without decoupling structure, high isolation is obtained between two antenna elements <−18 dB from 3.1–3.4 GHz and the overall size is 25×35×1.6mm^3. In [16], a triple notched UWB MIMO antenna with a size of 58×45×1.6mm^{3}is proposed. The structure uses a defected ground plane for the compactness and decoupling strips and a slotted ground plane for enhancing isolation which is > 15dB. Four-element MIMO antenna with a size of 80×80×1.52mm^3 is proposed in[17]. To improve the impedance bandwidth, it uses U-stab loaded on the radiator and defected ground plane, and by placing the elements orthogonally, isolation is improved to >15dB at the majority of the UWB. In [18], four-element MIMO consists of two alike slot dipoles and two alike planar monopoles with a total size of 70×41×0.8mm^3 which covers the whole UWB (3.1-10.6GHz) was developed with an isolation of >17dB . [11]reveals a 60×41×1mm^3 size compact MIMO antenna for UWB applications that achieves high isolation >20dB at the majority of the operating band due to the monopoles' complementary and asymmetrical structures, except > 10dB for 2.86–3.28 GHz . UWB MIMO antenna with double band rejection that has a size of 56×56×0.8mm^3 is depicted in [19]. The structure used rectangular and staircase-shaped stubs to obtain good isolation which is > 20dB at the majority of the band. On the other hand, in [20], The proposed compact four-element UWB-MIMO array was made up of four QSCA elements that are arranged anticlockwise to produce good impedance matching and 15 dB port-to-port isolation. Without employing any other decoupling techniques, the isolation is achieved. The total size is 40×40×1.6mm^3 .Recent MIMO antenna researches have mostly focused on the mutual coupling effect and studying several efficient strategies for reducing it. Surface current distribution is one of the critical factors in deciding the amount of mutual coupling between the antennas. In this work, a simple low-cost DGS based monopole patch antenna with triangular slot inside for UWB application is designed first, and then MIMO structures, which are two and four-element MIMO structures with different placements, are designed to come up with the desired MIMO antenna structure that has improved mutual coupling, better ECC and diversity gain. In the design, it is observed that mutual

coupling is reduced by the adjustment of the radiator element's orientation (placement). The development of the monopole antenna and simulation results are discussed in section 2, while MIMO antenna structures design, result analysis and evaluation are discussed in sections 3 and 4. All the simulations are done using CST software. Finally, in section 4.3, the suggested Quad-element MIMO antenna's simulated and measured results are discussed.

II. BASIC ANTENNA CONFIGURATION AND RESULT ANALYSIS

The UWB single-element antenna is derived from the design evolution of a full-ground-based rectangular monopole antenna fed by a 50 Ω microstrip line. Fig.1 (A-C) illustrates three different antenna designs in progress, from a simple patch to a DGS based patch with a triangular slot inside. The scaling or dimensions of an UWB antenna element for step-3 is indicated in Fig.2, and the parameters of the proposed UWB antenna are given in Table1.In the design ,FR-4 material with a dielectric constant (ε_o) of 4.3 and 1.6mm thickness is used as a substrate. In step-1, a simple rectangular microstrip element with a microstrip-line feeding technique is designed, while in step-2, a partial ground plane with two slots at $\lambda/2$ distance is designed, and in step-3, a triangular slot is introduced in the rectangular patch to achieve miniaturization and to cover the required ultra-wideband frequency. Since the key objective of the work is to propose a Quad-element UWB MIMO antenna with improved isolation, the design evolution of the three single-element antennas is evaluated according to their results.Fig.3 (a-d) presents the simulation results of the three antenna geometries to identify and select the desired antenna element.

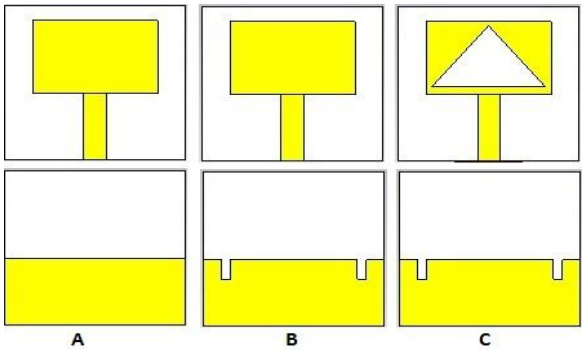

Figure 1.Monopole antenna designs: (A) Rectangular patch with full ground plane, (B) DGS based rectangular patch,(C) DGS based rectangular patch with triangular slot inside.

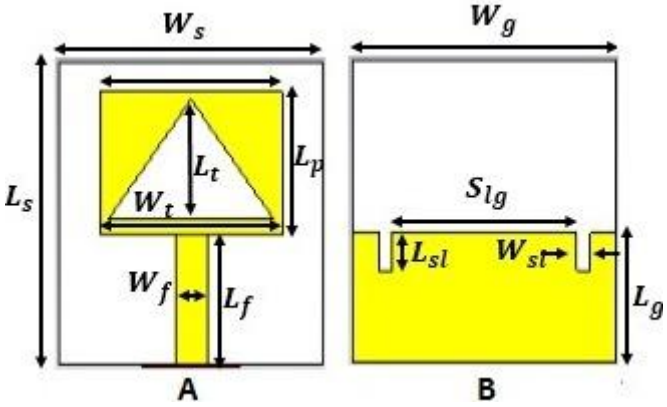

Figure 2.Scaling of UWB antenna :(A) Patch side, (B) Ground side.

TABLE 1. UWB MONOPOLE ANTENNA DIMENSIONS

Design specifications type	Dimensions	Design specifications type	Dimensions
substrate size($W_s \times L_s \times H_s$)	24×24×1.6mm3	Patch Slot width(W_t)	15.2mm
Full Ground size ($W_g \times L_{fg}$)	24×24mm2	Ground slot length(L_{sl})	3mm
Ground height (HG)	0.035mm	Ground slot width (W_{sl})	1.2mm
Partial ground plane size($W_g \times L_g$)	24×10.33mm2	Feed length (L_f)	10.33mm
Rectangular patch size($W_p \times L_p$)	16.6×11.33mm2	Feed width (W_f)	2.9mm
Patch Slot length(L_t)	9.5mm	Gap between ground slot(S_{lg})	15.2mm

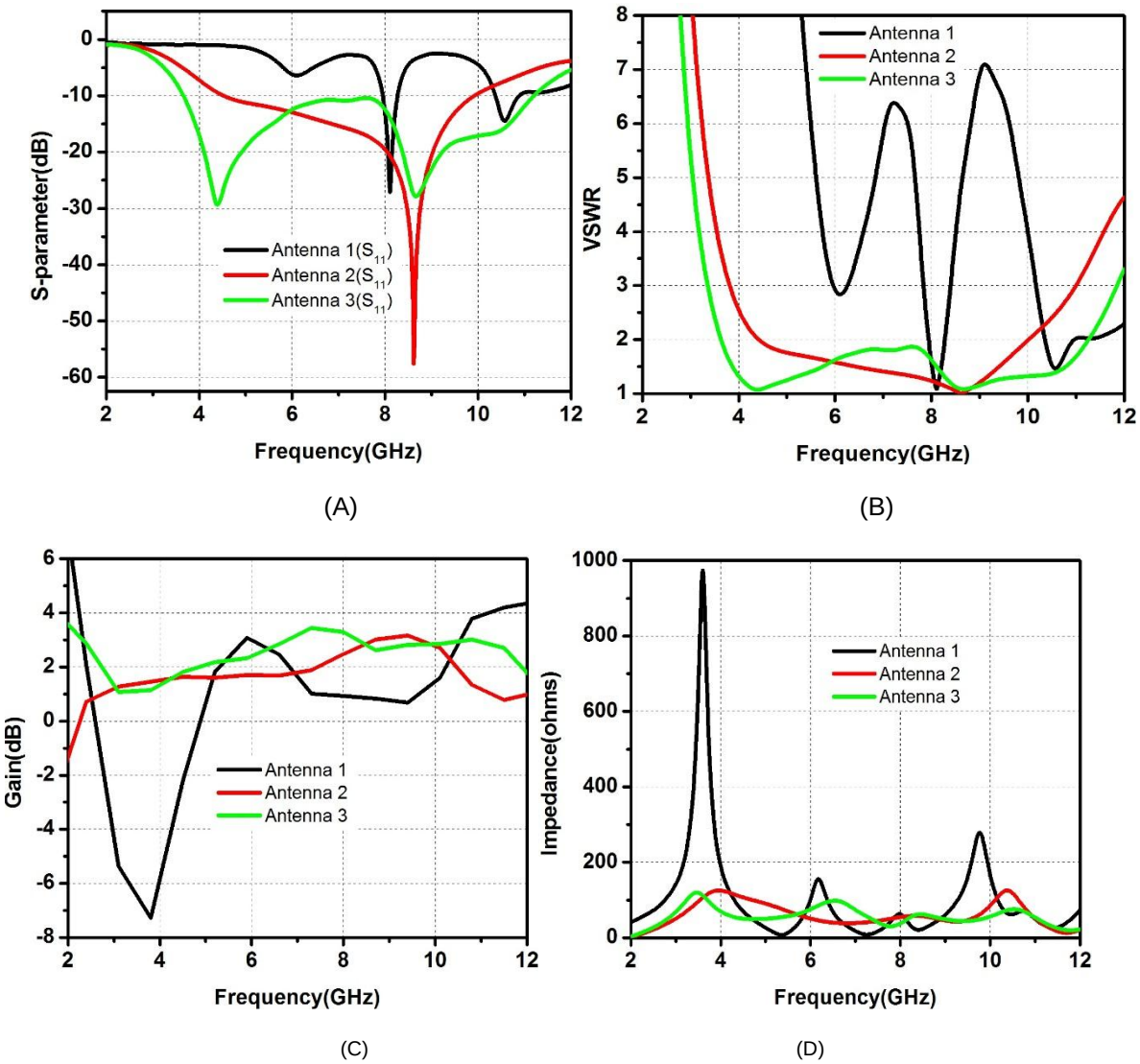

Figure.3. Simulation plots :(A) Reflection coefficient plot,(B) VSWR plot, (C) Gain plot,(D)Impedance plot.

As indicated in the plots, Step one antenna has an impedance bandwidth of 7.94-8.28GHz (4.1%) at ($|S_{11}|$< -10dB) with VSWR = 1.17 at a resonant frequency of 8.07 GHz, which is a narrow band. The second antenna has an impedance bandwidth of 4.55-9.29 GHz (68.49%) at ($|S_{11}|$ <-10dB), VSWR=1.04 at resonant frequency of 8.616 GHz, which indicates a broadband antenna. The broadband condition is happening because of the introduction of a defected ground plane, which completely altered the current distribution. The step-3 design provides an impedance bandwidth of 3.644-11.237GHz (101%) at ($|S_{11}|$<-10dB) with VSWR =1.1 at the resonant frequency. From the Gain Vs frequency plot, the peak gain in the operating band is 3.4dB. This is obtained from the third

antenna, while 3.03dB for the second antenna and 3dB for the first antenna. Fig. 3 (D) shows the impedance Vs. frequency plot, where the third antenna's curve nearly falls around the standard impedance value, which is 50 ohm (proper impedance matching effect). Therefore, from step by step geometric studies, step-3 monopole antenna design is preferable for the construction of MIMO antennas because of its ultra-wideband effect. Further, the proposed single element antenna was fabricated and tested using vector network analyzer. Fig.4.illustrates the simulation VS measurement result. Where it's$|S_{11}|$ measured values are almost similar to its simulation values.

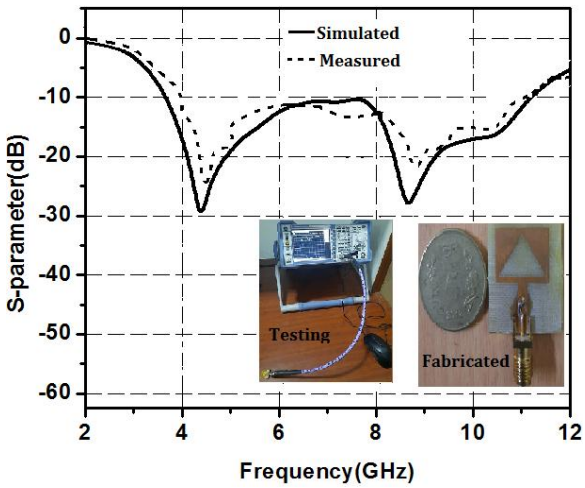

Figure 4. Measurement VS simulated result

III. MIMO ANTENNA DESIGN AND CONFIGURATION

For the two and four-element MIMO antenna structures, different antenna radiator orientations (placement) are presented in Fig. 5 (A-D). The proposed adjustments are according to the individual antenna elements' placement or layout. Fig. 5 (A) shows a two-element MIMO antenna-1.The radiators are placed on the same plane side by side with a gap of ~0.2 λ(7.4mm) and Fig. 5 (B) shows a two-element antenna-2. Here elements are oriented 180 degrees to each other with an inter-element gap of ~0.2λ (7.4 mm). Besides, the four-element MIMO antenna-1 and MIMO antenna-2 structures are presented in Fig. 5 (C) and (D), where, in the first MIMO, two antenna elements are placed in the same orientation with an inter-element gap of ~0.2λ (7.4 mm) to each other, and the remaining two elements are placed on the opposite side, oriented 180 degrees from the first two elements with an inter-element gap of ~0.12λ (4.67 mm). On the other hand, the second MIMO structure organizes two adjacent radiators orthogonal to each other where a single element has an inter-element gap of ~0.16λ (6.03mm) and ~0.13λ (5.03mm) to the two neighboring elements as indicated in the figure. The total sizes of the two-element MIMO antenna structures are 24mm×48mm×1.6mm each, while the four-element MIMO structures have a size of 48mm×48mm×1.6mm each.

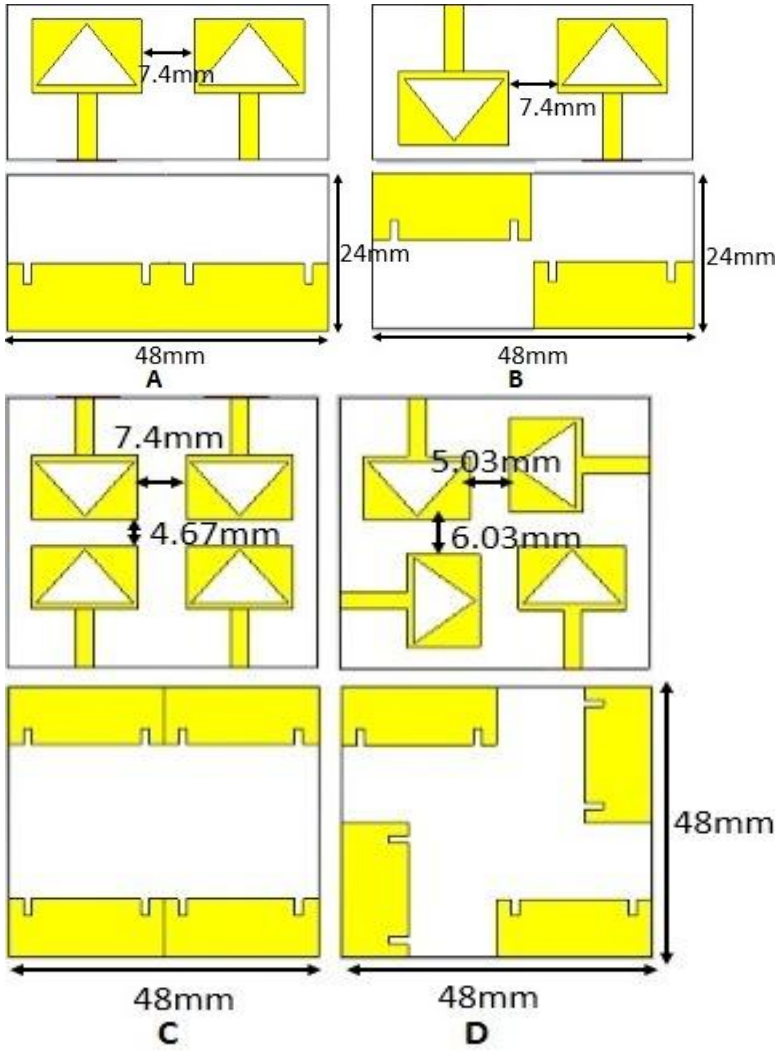

Figure 5. MIMO antennas top and bottom view: (A), (B) Two-element MIMO antenna orientaion-1& orientation-2, (C),(D) Four-element MIMO antenna orientaion-1& orientation-2.

IV. RESULT DISCUSSION

In this section, the simulation findings of the designed MIMO antennas, as well as the measurement results of the suggested four-element MIMO UWB antenna are discussed. The outcomes discussed include return loss, mutual coupling effect and diversity performance.

A. S-parameter

In this section, the return loss plot and isolation values are presented. The design geometries of both layouts are indicated in the previous section. Here, the comparative studies for both configurations based on their S-parameter results are discussed. Fig. 6 (A), shows the S-parameter simulation plot of the two-element MIMO antenna-1. Thus, the impedance bandwidth of this two-element MIMO antenna in this configuration is 3.47-11.00 GHz, and the majority of the band has < -12 dB mutual coupling effect. For the two-element MIMO antenna-2, when elements are oriented 1800 to each other, the S-parameter plot is revealed in Fig.6 (B) and the impedance bandwidth is 3.41 -11.09 GHz with the majority of its operating band has < -15 dB mutual coupling effect. In this way, the second MIMO configuration has slightly better bandwidth with enhanced isolation. Likewise, the four-element MIMO antenna simulation results are illustrated in Fig. 7 (A) and (B). The four-element MIMO antenna-1 return loss values are identical for all ports, which are 3.45-11.00 GHz with majority of its operating band's mutual coupling is < -15dB, while the four-element MIMO antenna-2 has a 3.60-11.42 GHz

impedance bandwidth and more than -20dB isolation for the majority of the operating band respectively.

B. Diversity performance

This study took into account the diversity performance of the designed configurations in order to properly evaluate the MIMO antenna. Thus, the envelope correlation coefficient (ECC) and diversity gain (DG) of all structures are compared, and the suggested quad-element antenna is also assessed against acceptable MEG and CCL criteria.

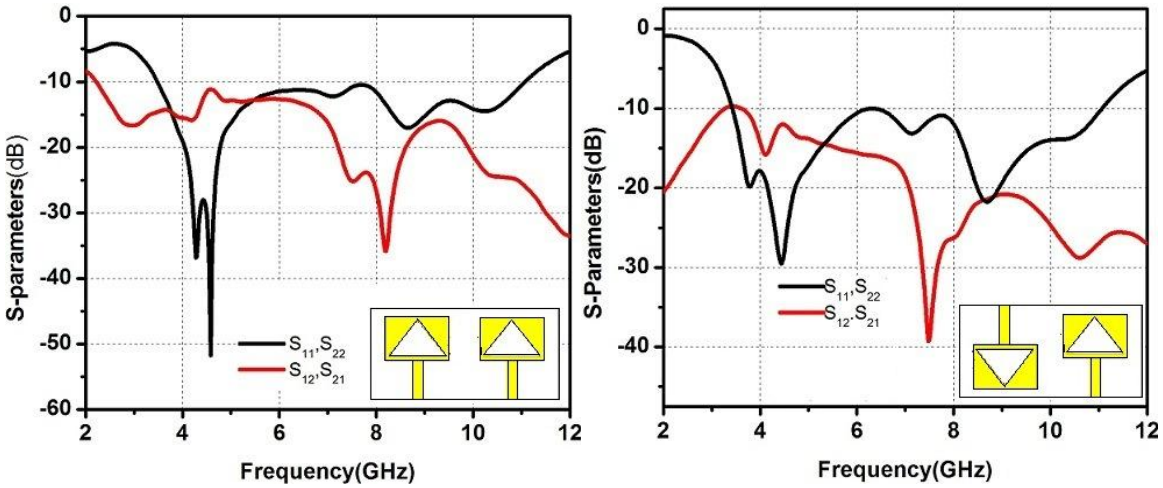

(A) (B)

Figure 6. Two element MIMO antenna S-parameter plots.(A)orientation-1,(B) orientation-2.

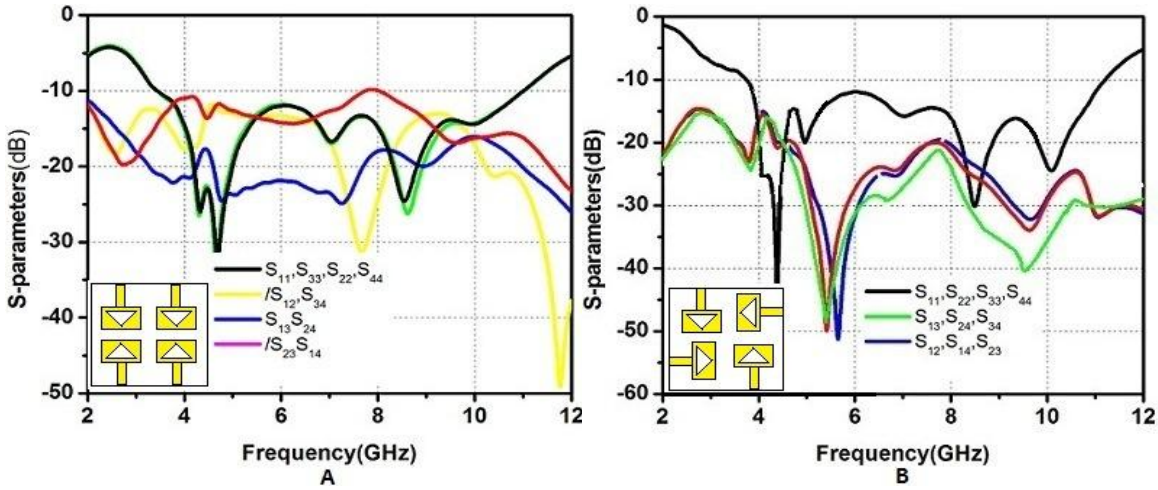

Figure 7. Four-element MIMO antenna S-parameter plots.(A) orientation-1,(B) orientation-2.

ECC is a measure of isolation between antenna elements that describes how two antenna elements' radiation patterns are independent. The signal to noise ratio of a MIMO antenna system, on the other hand, is assessed by diversity gain. In theory, it should be ten times that of the envelope correlation coefficient, but more than 9.5 is acceptable in practice. In general, maximum diversity gain is only attained when the envelope correlation coefficient is zero. The ECC is calculated using the S-parameter and the radiation pattern in Equations (1,2 and 3).[21]–[23].

$$\rho_{xy} = \frac{\left|S_{xx}^{*}S_{xy} + S_{yx}^{*}S_{yy}\right|^2}{\left(1-\left|S_{xx}\right|^2-\left|S_{yx}\right|^2\right)\left(1-\left|S_{yy}\right|^2-\left|S_{xy}\right|^2\right)} \quad [1]$$

Where S_{xy}, S_{yx} ,S_{yy} and S_{xx} are the scattered parameters and ρ_{xy} is ECC values.

$$\rho_e = \frac{\left|\iint_{4\pi} |F_1(\theta,\phi)* F_2(\theta,\phi)d\Omega\right|}{\iint_{4\pi}|F_1(\theta,\phi)|^2 d\Omega \iint_{4\pi}|F_2(\theta,\phi)|^2 d\Omega} \quad [2]$$

Where, $F_x(\theta,\emptyset)$ is the field radiation pattern when port x is excited.

Any MIMO antenna system's spectral efficiency is degraded by a larger value of the envelope correlation coefficient (ρ). As a result, achieving the lowest possible correlation coefficient is preferable. When the value of "ρ" approaches zero, a MIMO antenna system achieves near-perfect performance.

$$DG = 10\sqrt{1-(ECC)^2} \quad [3]$$

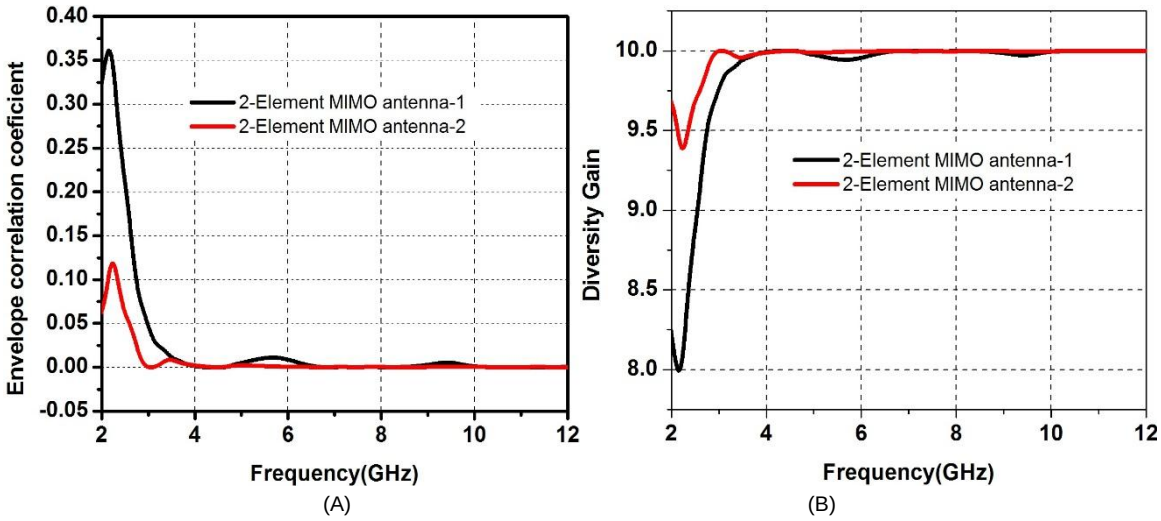

Figure 8. (A) ECC of two-element MIMO antenna orientation-1& -2, (B) DG of two-element MIMO antenna orientation-1& -2.

According to the results obtained in Fig 8 (A) & (B), the ECC and DG of orientation-1 are < 0.015 and > 9.91, while the ECC and DG of orientation-2 are < 0.006 and > 9.97 respectively. Fig. 9(a) and (b) show the ECC values of four-element MIMO antennas for both configurations, where, orientaion-1 has < 0.029 ECC value and orientation-2's ECC value is <0.006. Moreover, the DG value of the first structure is shown in Fig. 10 (A) and has a value of > 9.98 while the second structure has diversity gain > 9.99 as depicted in Fig. 10 (B). From the result indicators, the four-element MIMO antenna-2 has better diversity performance and isolation. That has to be taken to the fabrication of a prototype structure for result validation.

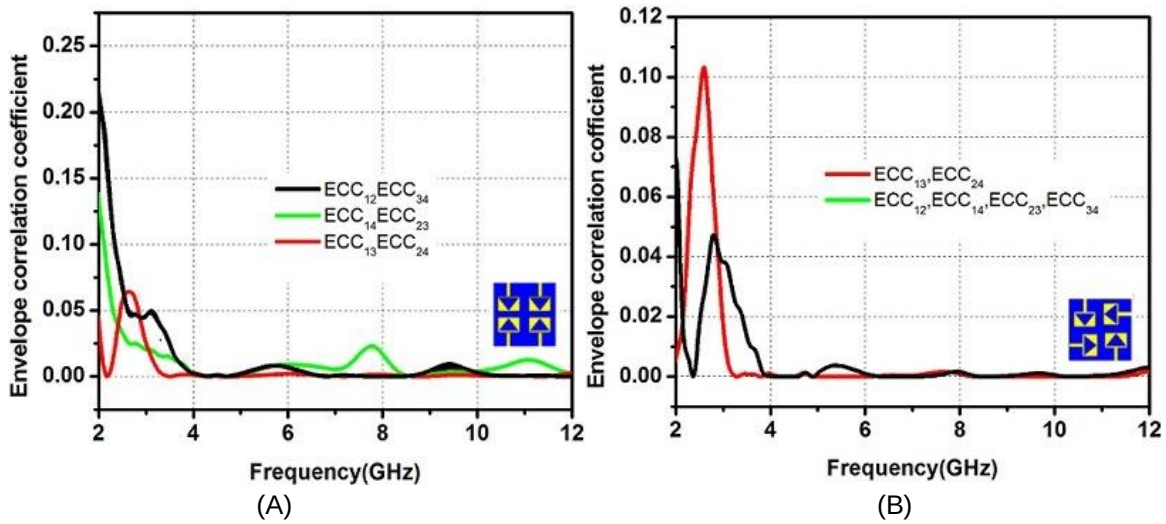

Figure 9.ECC simulation curves of four-element MIMO antenna:(A)orientation-1,(B)orientation-2.

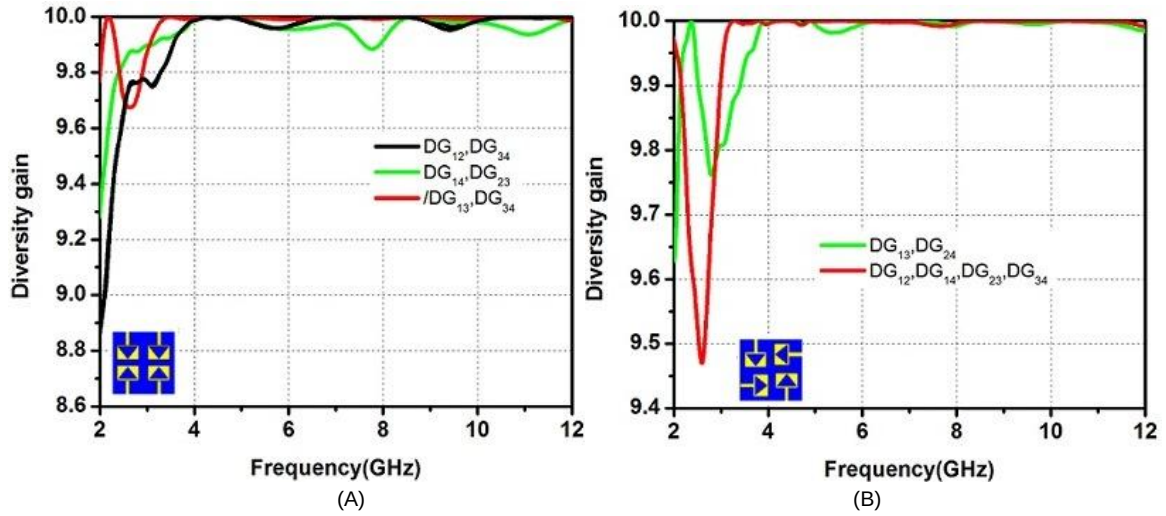

Figure 10.DG simulation curves of four-element MIMO antenna:(A)orientation-1,(B)orientation-2

The four-element MIMO antenna-2 is further investigated using the mean effective gain (MEG) and it is calculated using equation (4). For good diversity performance, the practical standard followed is that MEG should be −3 ≤ MEG (dB) <-12 [24]. Thus, as we can observe from MEG plots in Fig.11 (A), all are between -3dB and -12dB

$$MEG_i = 0.5\left(1-\sum_{j=1}^{k}\left|S_{ij}\right|\right)[4]$$

Farthermore,CLL is another significant diversity performance measure for MIMO antenna analysis. It refers to the highest possible information transmission rate at which the signal can be easily conveyed without considerable loss. The following equations are used to compute the CCL[22].

$$CCL = -\log_2 \det(\partial)[5]$$

$$\partial = \begin{vmatrix} \partial_{11} & \partial_{12} & \partial_{13} & \partial_{14} \\ \partial_{21} & \partial_{22} & \partial_{23} & \partial_{24} \\ \partial_{31} & \partial_{32} & \partial_{33} & \partial_{34} \\ \partial_{41} & \partial_{42} & \partial_{43} & \partial_{44} \end{vmatrix}$$

$$\partial_{xx} = 1 - \left(\sum_{y=1}^{M} \left| S_{xy} \right|^2 \right) \text{where, } \partial_{xy} = -\left| S_{xx}^{*} S_{xy} + S_{yy}^{*} S_{yx} \right|$$

CCL computed for the four-element MIMO antenna orientation-2 is depected in Fig.11(B). It is observed that the CCL is below 0.1 bits/sec/Hz, which is agreed with the standard value of CCL to be <0.4 bits/sec/Hz. The capacity of a MIMO antenna increases as the number of antennas grows.

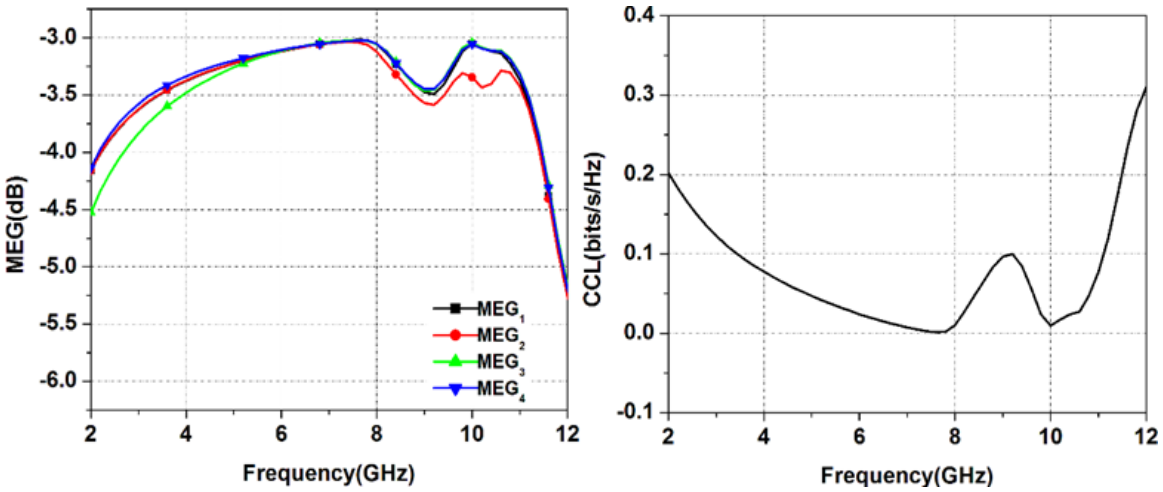

(A) (B)

Figure 11.Simulated results :(a) MEG, (b) CLL

The surface current distribution of the suggested MIMO antenna is revealed in Fig.12. Surface current analysis is carried out at 4.38GHz, which is one of the resonant frequencies. Antenna radiator-1 is excited at this resonance frequency, and the other radiators are regarded to be suited to the 50 ohm impedance. This method is used to look into the antenna parts that affect the MIMO structure's radiation characteristics and reveal the amount of coupling between radiator elements. It is clear that the surface current density is highest on the triangular slot's edges, around the feed line, and a significant amount also appears on the defected ground structure.

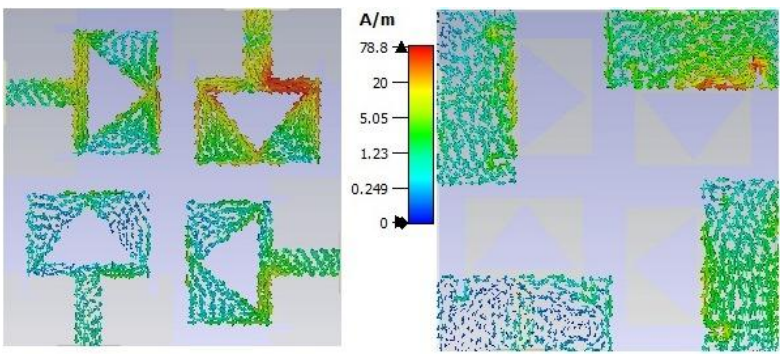

(A) (B)

Fig.12. Surface current distribution :(a) patch side, (b) ground side.

The comparison table of the designed MIMO antennas is stated in Table 2. From this table, two-element MIMO antenna-2's element isolation is better than two-element MIMO antenna-1 by 3 dB. But for the four-element MIMO antenna, MIMO antenna-2 isolation is better than MIMO antenna-1by 5 db. Therefore, MIMO Antenna-2 is more efficient compared to the MIMO Antenna-1 in both cases.

TABLE 2.SIMULATION RESULT COMPARISONS ON THE DESIGNED MIMO ANTENNA STRUCTURES

MIMO structure type		MC (on majority Of the band)	Impedance Bandwidth	ECC	DG
Number of elements	Orientation				
2-element	MIMO-1	<-12dB	3.47GHz-11.00GHz	<0.015	>9.91
	MIMO-2	<-15dB	3.41GHz-11.09GHz	<0.006	>9.97
4-element	MIMO-1	<-15dB	3.45GHz-11.00GHz	<0.029	>9.80
	MIMO 2	<-20dB	3.60GHz-11.42GHz	<0.006	>9.90

C.Measurement and simulation results discussion

The fabricated prototype of the MIMO antenna-2 is depicted in Fig. 13. The experimental results [25], [26]are tested using a vector network analyzer and compared with the simulated results as illustrated in the graphs of Fig .15 (A-C). It operates from 3.5 to 11.2GHz and has good element isolation with some un-smoothness in the curves and a little deviation from the simulation results. Besides, the elements have a less mutual coupling effect, as can be noticed from the curves, with the majority of the band falling below <-20dB. Farther more, the measured ECC and DG values almost agree with the simulated results. The slight mismatching effect in all curves is due to fabrication imperfection, soldering of connectors that produces losses.

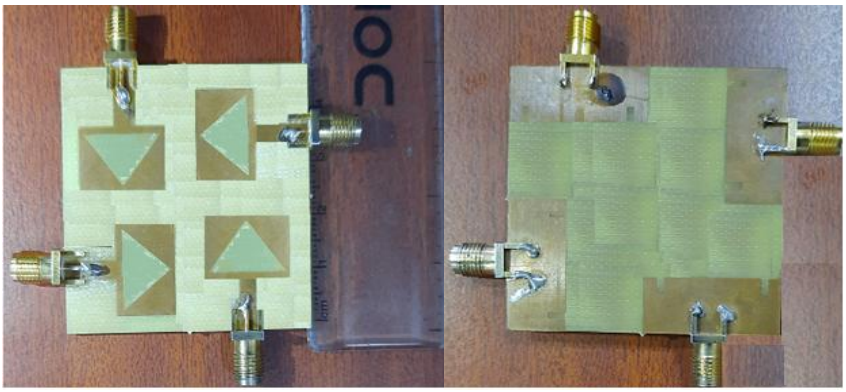

(A) (B)

Figure 13.Prototype. (A) Top view, (B) Bottom view.

Comparisons table i.e. Table 3 summarizes results comparisons among recently proposed MIMO antenna systems, and our design has comparatively high isolation, as can be shown, low ECC value and nearly 10 diversity gain and is small in size. But, the peak gain is moderate compared to the indicated references. Therefore, the proposed structure will be important for UWB MIMO application.

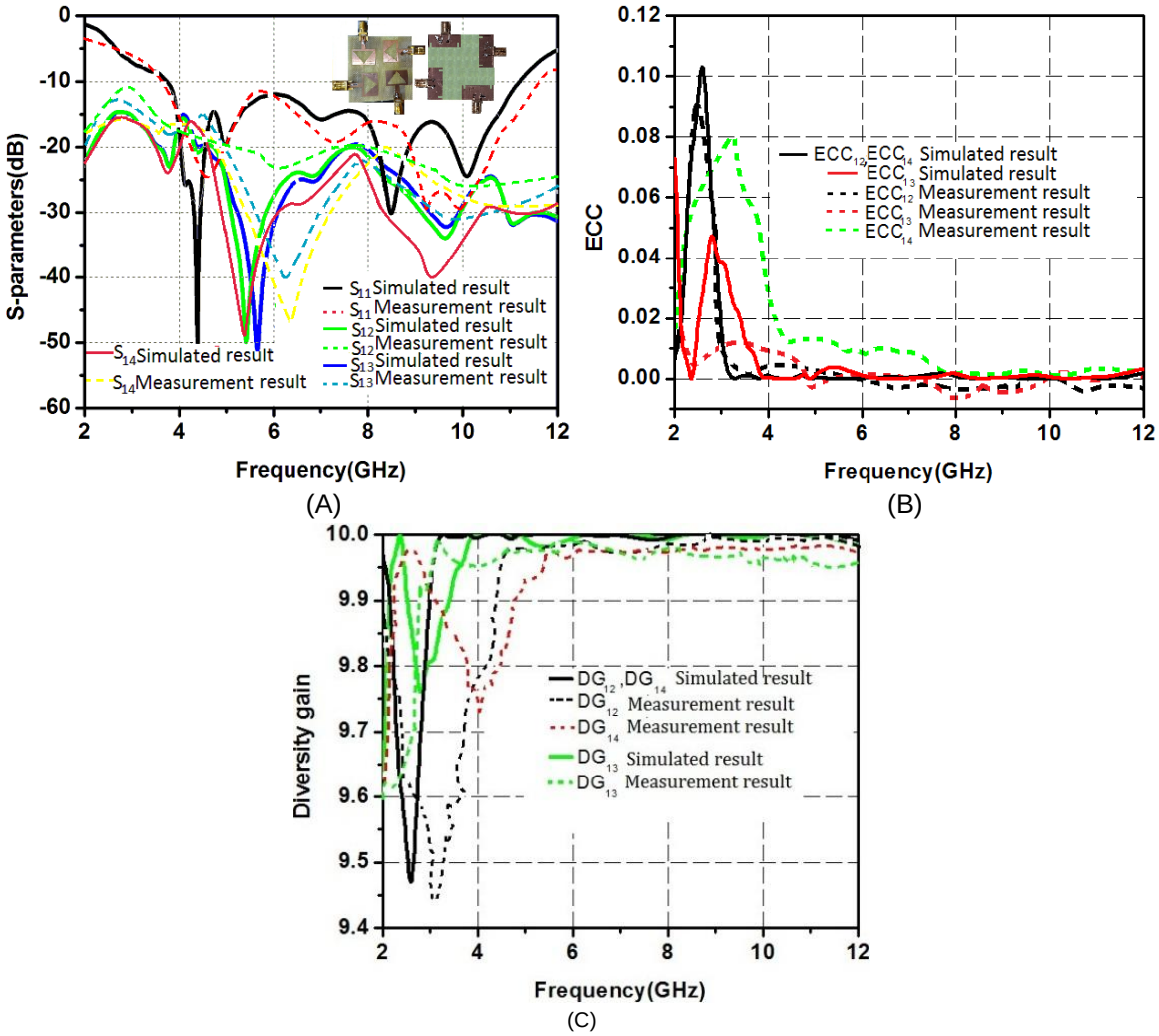

Figure14. Simulated Vs measured values :(A) S-parameter plot, (B) ECC plot,(C)diversity gain Plot.

The radiation pattern depicts the angular distribution of radiated power density in the far field. According to IEEE standards, the E-plane of an antenna is the plane containing the electric field vector and the maximum radiation direction or it is kept aligned along the desired orientation[27], while the H-plane is the plane containing the magnetic field vector and the maximum radiation direction .The simulated and measured E- and H-plane radiation patterns at 4.38, 8.5, and 10.5 GHz are shown in Fig.15 (A-C).The measured results are suited with the simulated result except for slight deviation as revealed in the radiation plot.

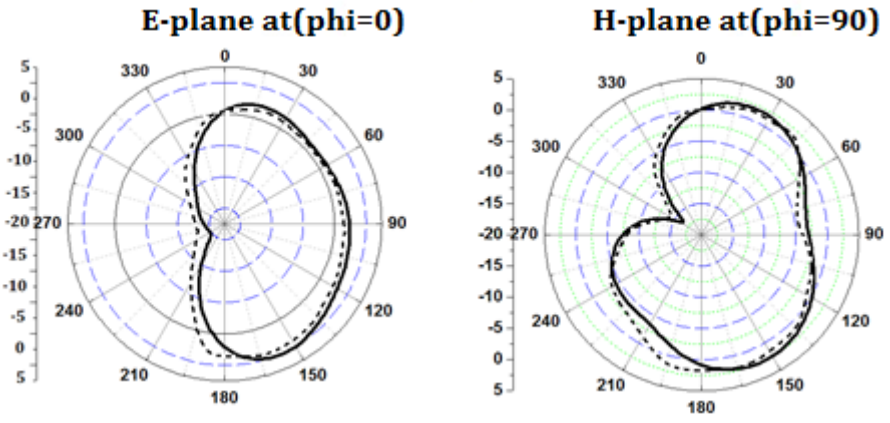

(A)

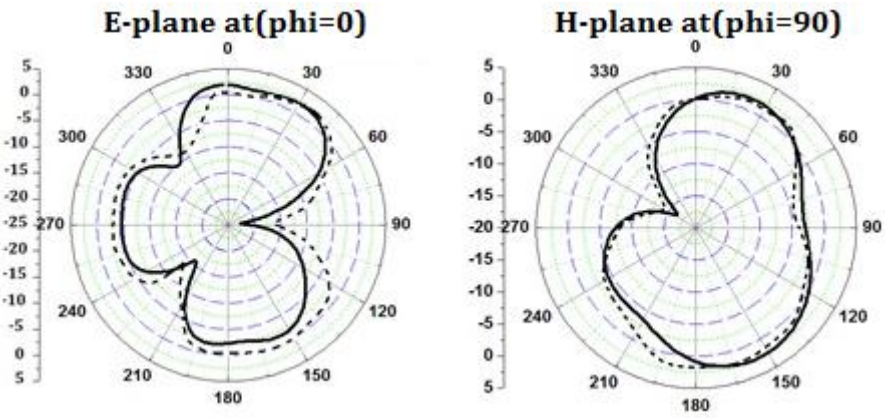

(B)

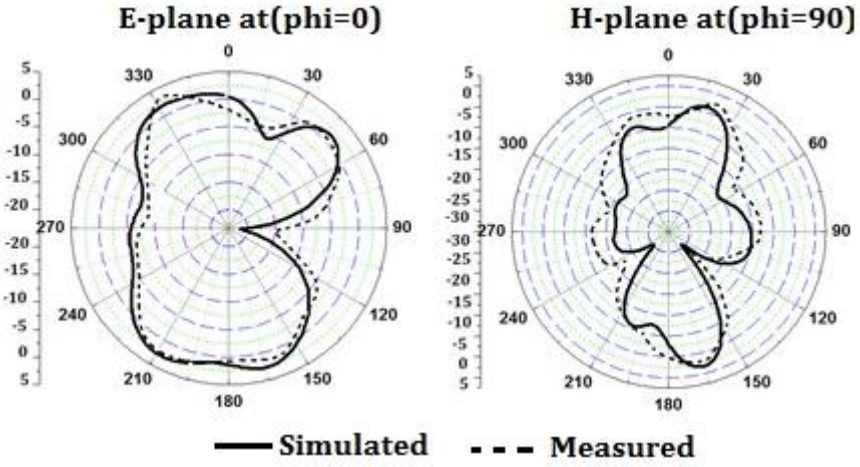

(C)

Figure 15. Measured Vs simulated radiation patterns: (A) 4.38 GHz; (B) 8.5 GHz,(C) 10.5 GHz

TABLE 3.COMPARISON OF THE PROPOSED STRUCTURE WITH OTHER ANTENNA

Reference	Number radiating elements	Impedance BW(<10dB) in GHz	MC(on majority Of the band)	Size (mm3)	ECC	D.G.
[12]	2	3.00-10.90	<-20	30×50×1.6	<0.06	>9.6
[13]	2	3.00-12.00	<-20dB	66.2×66.2×1.6	<0.005	_
[14]	2	3.00-11.00	<-20dB	40×80×1.6	_	_
[10]	2	1.85-10.60	<-10dB	50×90×1.52	<0.16	>9.5
[15]	2	3.10-3.40	<-18dB	25×35×1.6	<0.005	-
[16]	2	3.10-11.00	<-15dB	58×45×1.6	<0.5	_
[17]	2/4	3.18-11.50	<-15dB	80×80×1.52	<0.015	>9.98
[18]	4	3.10-10.60	<17dB	70×41×0.8	<0.012	>9.95
[11]	4	3.10-10.60	<-20dB	60×41×1.0	<0.250	-
[19]	4	3.20-10.70	<-20dB	56×56×1.6	-	-
[20]	4	2.95-12.10	<-15dB	40×40×0.8	<0.04	-
Proposed work	4	3.20-11.20	<-20dB	48×48×1.6	<0.006	>9.99

V. CONCLUSION

In this paper, a quad-element MIMO antenna is proposed for UWB communication. The miniaturization and high performance of the basic monopole antenna is achieved by introducing defected ground structure and slots on the patch. Different placements (orientations) both for two–element and four-element MIMOs are analyzed and compared using the results obtained from the simulation. The MIMO structures are investigated for best performance in return loss, mutual coupling effect, and diversity performance. It has been discovered that the Quad-element MIMO antenna with orthogonal placement operates in the UWB range with better element isolation and better diversity performance. Except for slight deviations and un-smoothness of the curves, the suggested Quad-element MIMO antenna's measured and simulated results are in good accord. Consequently, the overall dimension of the proposed Quad-element MIMO antenna is $48\times48\times1.6mm^3$ and it could be a good fit for UWB-MIMO wireless communication applications

REFERENCES

[1] Z. Khan, A. Razzaq, J. Iqbal, A. Qamar, and M. Zubair, "Double circular ring compact antenna for ultra-wideband applications," IET Microw. Antennas Propag., vol. 12, no. 13, pp. 2094–2097, Oct. 2018, doi: 10.1049/iet-map.2018.5245.

[2] K. Kamakshi, J. A. Ansari, A. Singh, M. Aneesh, and A. K. Jaiswal, "A novel ultrawideband toppled trapezium-shaped patch antenna with partial ground plane," Microw. Opt. Technol. Lett., vol. 57, no. 8, pp. 1983–1986, Aug. 2015, doi: 10.1002/mop.29231.

[3] D. Venkatachalam and M. Govindasamy, "A miniaturized planar antenna with defective ground structure for UWB applications," IEICE Electron. Express, vol. 16, no. 14, pp. 20190242–20190242, 2019, doi: 10.1587/elex.16.20190242.

[4] M. K. Khandelwal, B. K. Kanaujia, and S. Kumar, "Defected Ground Structure: Fundamentals, Analysis, and Applications in Modern Wireless Trends," Int. J. Antennas Propag., vol. 2017, pp. 1–22, 2017, doi: 10.1155/2017/2018527.

[5] S. Pramono and B. B. Subagio, "Mutual Coupling Reduction & Bandwidth Enhancement Using a Simple Folded Slot-PartialGround Plane in Dualband MIMO Antenna," in 2018 International Seminar on Intelligent Technology and Its Applications (ISITIA), Bali, Indonesia, Aug. 2018, pp. 19–22. doi: 10.1109/ISITIA.2018.8711213.

[6] K. Wei, J. Y. Li, L. Wang, R. Xu, and Z. J. Xing, "A New Technique to Design Circularly Polarized Microstrip Antenna by Fractal Defected Ground Structure," IEEE Trans. Antennas Propag., vol. 65, no. 7, pp. 3721–3725, Jul. 2017, doi: 10.1109/TAP.2017.2700226.

[7] N. Kishore, A. Prakash, and V. S. Tripathi, "A multiband microstrip patch antenna with defected ground structure for its applications," Microw. Opt. Technol. Lett., vol. 58, no. 12, pp. 2814–2818, Dec. 2016, doi: 10.1002/mop.30151.

[8] A. Ahmed, "Electromagnetic Band Gap Coupled Microstrip Antenna for UWB Applications," IOSR J. Electron. Commun. Eng., vol. 2, no. 6, pp. 01–03, 2012, doi: 10.9790/2834-0260103.

[9] B. P. Smyth, S. Barth, and A. K. Iyer, "Dual-Band Microstrip Patch Antenna Using Integrated Uniplanar Metamaterial-Based EBGs," IEEE Trans. Antennas Propag., vol. 64, no. 12, pp. 5046–5053, Dec. 2016, doi: 10.1109/TAP.2016.2618854.

[10] S. K. Dhar and M. S. Sharawi, "A UWB semi-ring MIMO antenna with isolation enhancement," Microw. Opt. Technol. Lett., vol. 57, no. 8, pp. 1941–1946, Aug. 2015, doi: 10.1002/mop.29245.

[11] X.-L. Liu, Z.-D. Wang, Y.-Z. Yin, J. Ren, and J.-J. Wu, "A Compact Ultrawideband MIMO Antenna Using QSCA for High Isolation," IEEE Antennas Wirel. Propag. Lett., vol. 13, pp. 1497–1500, 2014, doi: 10.1109/LAWP.2014.2340395.

[12] E. Wang, W. Wang, X. Tan, Y. Wu, J. Gao, and Y. Liu, "A UWB MIMO slot antenna using defected ground structures for high isolation," Int. J. RF Microw. Comput.-Aided Eng., vol. 30, no. 5, May 2020, doi: 10.1002/mmce.22155.

[13] R. V. S. R. Krishna and R. Kumar, "A Dual-Polarized Square-Ring Slot Antenna for UWB, Imaging, and Radar Applications," IEEE Antennas Wirel. Propag. Lett., vol. 15, pp. 195–198, 2016, doi: 10.1109/LAWP.2015.2438013.

[14] M. Li, Y. Yu, and T. Hong, "A Compact UWB MIMO Antenna with Extended Ground to Reduce Coupling," in 2019 IEEE International Symposium on Broadband Multimedia Systems and Broadcasting (BMSB), Jeju, Korea (South), Jun. 2019, pp. 1–3. doi: 10.1109/BMSB47279.2019.8971882.

[15] Y. Wu, K. Ding, B. Zhang, J. Li, D. Wu, and K. Wang, "Design of a Compact UWB MIMO Antenna without Decoupling Structure," Int. J. Antennas Propag., vol. 2018, pp. 1–7, 2018, doi: 10.1155/2018/9685029.

[16] N. Jaglan, S. D. Gupta, B. K. Kanaujia, S. Srivastava, and E. Thakur, "TRIPLE BAND NOTCHED DG-CEBG STRUCTURE BASED UWB MIMO/DIVERSITY ANTENNA," Prog. Electromagn. Res. C, vol. 80, pp. 21–37, 2018, doi: 10.2528/PIERC17090702.

[17] M. N. Hasan, S. Chu, and S. Bashir, "A DGS monopole antenna loaded with U-shape stub for UWB MIMO applications," Microw. Opt. Technol. Lett., vol. 61, no. 9, pp. 2141–2149, Sep. 2019, doi: 10.1002/mop.31877.

[18] L. S. Yang, M. Xu, and C. Li, "Four-Element MIMO Antenna System for UWB Applications," Radioengineering, vol. 27, no. 1, pp. 60–67, Apr. 2019, doi: 10.13164/re.2019.0060.

[19] Mengyuan Lin and Zengrui Li, "A compact 4 × 4 dual band-notched UWB MIMO antenna with high isolation," in 2015 IEEE 6th International Symposium on Microwave, Antenna, Propagation, and EMC Technologies (MAPE), Shanghai, China, Oct. 2015, pp. 126–128. doi: 10.1109/MAPE.2015.7510281.

[20] J.-F. Yu, X. L. Liu, X.-W. Shi, and Z. Wang, "A COMPACT FOUR-ELEMENT UWB MIMO ANTENNA WITH QSCA IMPLEMENTATION," Prog. Electromagn. Res. Lett., vol. 50, pp. 103–109, 2014, doi: 10.2528/PIERL14110804.

[21] K. S. Sultan and H. H. Abdullah, "PLANAR UWB MIMO-DIVERSITY ANTENNA WITH DUAL NOTCH CHARACTERISTICS," Prog. Electromagn. Res. C, vol. 93, pp. 119–129, 2019, doi: 10.2528/PIERC19031202.

[22] W. M. Abdulkawi, W. A. Malik, S. U. Rehman, A. Aziz, A. F. A. Sheta, and M. A. Alkanhal, "Design of a Compact Dual-Band MIMO Antenna System with High-Diversity Gain Performance in Both Frequency Bands," Micromachines, vol. 12, no. 4, p. 383, Apr. 2021, doi: 10.3390/mi12040383.

[23] A. A. Ibrahim, M. A. Abdalla, and Z. Hu, "Compact ACS-fed CRLH MIMO antenna for wireless applications," IET Microw. Antennas Propag., vol. 12, no. 6, pp. 1021–1025, May 2018, doi: 10.1049/iet-map.2017.0975.

[24] M. Khalid et al., "4-Port MIMO Antenna with Defected Ground Structure for 5G Millimeter Wave Applications," Electronics, vol. 9, no. 1, p. 71, Jan. 2020, doi: 10.3390/electronics9010071.

[25] S. K. Oruganti, A. Khosla, and T. G. Thundat, "Wireless Power-Data Transmission for Industrial Internet of Things: Simulations and Experiments," IEEE Access, vol. 8, pp. 187965–187974, 2020, doi: 10.1109/ACCESS.2020.3030658.

[26] S. K. Oruganti et al., "Experimental Realization of Zenneck Type Wave-based Non-Radiative, Non-Coupled Wireless Power Transmission," Sci. Rep., vol. 10, no. 1, p. 925, Dec. 2020, doi: 10.1038/s41598-020-57554-1.

[27] J. Malik, S. K. Oruganti, S. Song, N. Y. Ko, and F. Bien, "Electromagnetically induced transparency in sinusoidal modulated ring resonator," Appl. Phys. Lett., vol. 112, no. 23, p. 234102, Jun. 2018, doi: 10.1063/1.5029307.